

Article

# Solid-Phase Extraction of Catechins from Green Tea with Deep Eutectic Solvent Immobilized Magnetic Molybdenum Disulfide Molecularly Imprinted Polymer

Wanwan Ma and Kyung Ho Row \* 

Department of Chemistry and Chemical Engineering, Inha University, Incheon 402-701, Korea; wanwanma@inha.edu

\* Correspondence: rowkho@inha.ac.kr; Tel.: +82-32-860-7470

Academic Editor: Saverio Bettuzzi

Received: 10 December 2019; Accepted: 8 January 2020; Published: 9 January 2020



**Abstract:** A type of molecular-imprinted polymer with magnetic molybdenum disulfide as a base and deep eutectic solvent as a functional monomer ( $\text{Fe}_3\text{O}_4@\text{MoS}_2@\text{DES-MIP}$ ) was prepared with surface molecular imprinting method. It was applied as the adsorbent for the selective recognition and separation of (+)-catechin, (–)-epicatechin, (–)-epigallocatechin, (–)-epicatechin gallate, and (–)-epigallocatechin gallate in green tea in the process of magnetic solid-phase extraction (MSPE) combined with high-performance liquid chromatography (HPLC). The structure of  $\text{Fe}_3\text{O}_4@\text{MoS}_2@\text{DES-MIP}$  was characterized by Fourier transform infrared spectroscopy and field emission scanning electron microscopy. The adsorption properties and selective recognition ability on (–)-epigallocatechin gallate and the other four structural analogues were examined and compared. The results show that the polymer has excellent selective recognition ability for (–)-epigallocatechin gallate, and its adsorption capacity was much higher than that of structural analogues. The  $\text{Fe}_3\text{O}_4@\text{MoS}_2@\text{DES-MIP}$  not only has the special recognition ability to template a molecule, but also can be separated by magnets with high separation efficiency and can be used in MSPE.

**Keywords:** molecular imprinted polymers; magnetic solid-phase extraction; deep eutectic solvents; molybdenum disulfide; catechins

## 1. Introduction

Green tea is considered a healthy drink and has become one of the most widely consumed beverages [1]. In addition, it has been used in the food, pharmaceutical, chemical, and light industries for thousands of years, especially in Asia, because of its numerous benefits, such as cancer prevention, inhibition of oxidation, and lowering blood pressure [2–4]. Catechins are the unique components of green tea that endow green tea with its physiological effects [5,6]. (+)-Catechin (C), (–)-epicatechin (EC), (–)-epigallocatechin (EGC), (–)-epicatechin gallate (ECG), and (–)-epigallocatechin gallate (EGCG) are the main catechins in green tea. Their excellent anti-oxidation, anti-cancer, and anti-cancer activities have prompted research into the separation and purification of those bioactive compounds [7–9]. The separation and purification technologies include distillation, freezing clarification, organic solvent extraction, and ion exchange. High purity catechins can be obtained through a combination of the above technologies [10]. On the other hand, these techniques do not meet the requirements of the separation and purification of trace analogs in complex systems, and these analogs are often difficult to analyze.

Molecular imprinting technology (MIT) is a type of molecular specific recognition technology that has developed rapidly in recent years [11]. The preparation technology of molecularly imprinted polymers (MIP) can be divided into two categories: embedding method [12] and surface molecularly imprinting method [13,14]. Encapsulation includes mainly bulk polymerization, suspension polymerization, emulsion polymerization, and precipitation polymerization. On the other hand, with the development of molecularly imprinted technology, the molecularly imprinted polymers prepared by the encapsulation method have the disadvantages of a large particle size, few imprinted dots, and few binding sites [15–17]. The surface molecularly imprinted method can be divided into the sacrificial carrier method, polymerization plus membrane method, and chemical grafting method [18]. The molecularly imprinted polymer synthesized by this method has more effective imprinting points owing to its large specific surface area. Moreover, its imprinting layer is thinner than that prepared by the embedding method, with faster desorption and adsorption rates, and template leakage can be eliminated. Because of the above advantages, surface molecularly imprinted technology has attracted increasing attention. This technology has broad application prospects in drug separation, sensors, solid-phase extraction, and food safety detection.

Molybdenum disulfide ( $\text{MoS}_2$ ) is a two-dimensional layered material with a natural adjustable bandgap and its monolayers are bonded via weak van der Waals forces and exhibit strong covalent S-Mo-S bonds in the plane [19].  $\text{MoS}_2$  is considered an appropriate candidate as an alternative to graphene owing to its similar structure, and it has begun to be applied to MIP processes [20,21]. Magnetic  $\text{MoS}_2$  by combining  $\text{Fe}_3\text{O}_4$  with  $\text{MoS}_2$  improved the potential of this material as an absorbent for magnetic solid-phase extraction (MSPE) because it could be easily and directly collected with an extra magnet.

Deep eutectic solvents (DESs) are a new type of ionic liquid-like solvent that has attracted attention because of their excellent physical and chemical properties, such as better chemical stability, designability, and recyclability, than ionic liquids (ILs) [22,23]. Moreover, DESs can be produced using inexpensive raw materials and offer environmental protection and simple synthesis processes [24–26]. Therefore, DESs are considered green solvents, as important as the ionic liquids, to replace traditional organic solvents. According to previous research [27,28], several types of DES have been applied as the functional monomer in the synthesis of MIPs, whereas a DES with the composition of vinyl-pyrrolidone (VP) and malonic acid (MA), which exhibits biocompatibility and new functions, has rarely been applied and discussed [29].

In this paper, a magnetic surface molecularly imprinted polymer (MIP) was prepared using a surface molecular imprinting method with nanometer magnetic  $\text{MoS}_2$  as a carrier; EGCG, as the template molecule; DES consisting of VP and MA as the functional monomer; and glycol dimethacrylate as the cross-linking agent. The structure of the DES-based MIP ( $\text{Fe}_3\text{O}_4@ \text{MoS}_2@ \text{DES-MIPs}$ ) was characterized, and its extraction and selective recognition ability for EGCG is discussed.

## 2. Results and Discussion

### 2.1. Characterization of $\text{Fe}_3\text{O}_4@ \text{MoS}_2@ \text{DES-MIP}$

The DES,  $\text{Fe}_3\text{O}_4@ \text{MoS}_2$ -MPS base and  $\text{Fe}_3\text{O}_4@ \text{MoS}_2@ \text{DES-MIP}$  with DES functional monomer were analyzed by FTIR spectroscopy, and the FTIR spectra is given in Figure 1.  $\text{MoS}_2$  showed a very strong characteristic stretching vibration peak of Mo-S around  $600 \text{ cm}^{-1}$ , which also can be observed from the spectrums of  $\text{Fe}_3\text{O}_4@ \text{MoS}_2$ -MPS and  $\text{Fe}_3\text{O}_4@ \text{MoS}_2@ \text{DES-MIP}$ , which is evidence of the successful coating of  $\text{MoS}_2$  at those two materials.  $\text{Fe}_3\text{O}_4@ \text{MoS}_2$ -MPS and  $\text{Fe}_3\text{O}_4@ \text{MoS}_2@ \text{DES-MIPs}$  both have absorption peaks around  $575 \text{ cm}^{-1}$ , which is the characteristic absorption peak of Fe-O in  $\text{Fe}_3\text{O}_4$ ; it is speculated that the  $\text{Fe}_3\text{O}_4$  formed on the surface of  $\text{MoS}_2$  polymer was successful. The peaks arounds  $1200 \text{ cm}^{-1}$  and  $1500 \text{ cm}^{-1}$  were assigned to the C-N stretching vibration and C-N bending vibration, indicating the successful preparation of DES from VP and MA. In addition, the strong broad peak around  $3000 \text{ cm}^{-1}$  of O-H vibration peak was attributed to a large number of hydrogen

bonds formed in DES. These bands confirmed the presence of the DES and base of  $\text{Fe}_3\text{O}_4@MoS_2$  in the  $\text{Fe}_3\text{O}_4@MoS_2@DES-MIP$  structure.

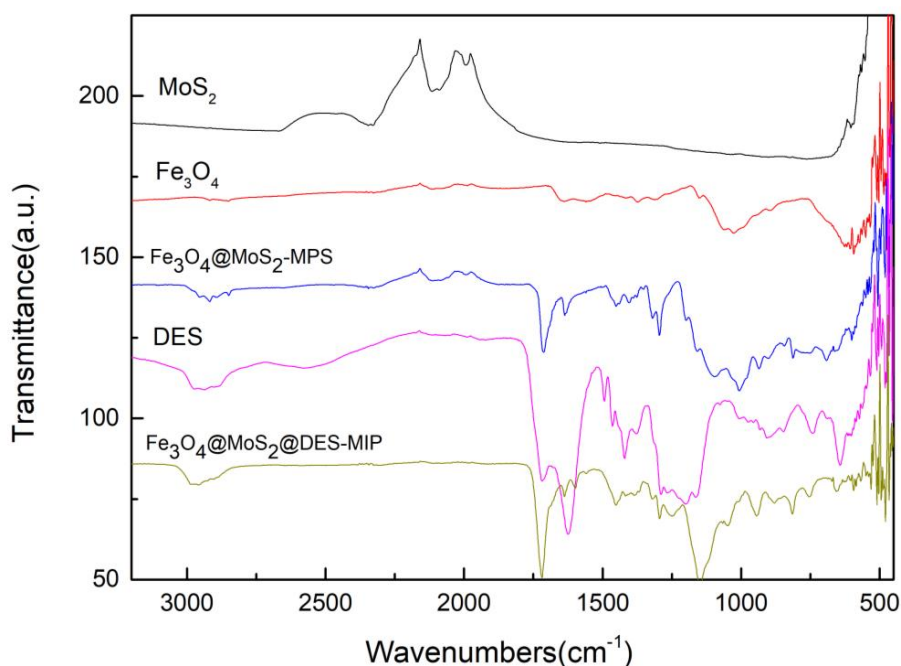


**Figure 1.** FTIR spectra of  $\text{MoS}_2$ ,  $\text{Fe}_3\text{O}_4$ ,  $\text{Fe}_3\text{O}_4@MoS_2$ -MPS, DES, and  $\text{Fe}_3\text{O}_4@MoS_2@DES-MIP$ .

The FESEM (field emission scanning electron microscopy) images of  $\text{MoS}_2$ ,  $\text{Fe}_3\text{O}_4@MoS_2$ , and  $\text{Fe}_3\text{O}_4@MoS_2@DES-MIP$  are shown in Figure 2, and the structural characteristics of the polymer can be clearly seen. As we can see from the figure of  $\text{MoS}_2$ , the morphology of  $\text{MoS}_2$  was a schistose structure and the particle size distribution was uniform. It can be seen from  $\text{Fe}_3\text{O}_4@MoS_2$  that there was a thick crust of  $\text{Fe}_3\text{O}_4$  wrapped on the surface of  $\text{MoS}_2$ , indicating that  $\text{Fe}_3\text{O}_4@MoS_2$  has been successfully prepared. As shown in the part of  $\text{Fe}_3\text{O}_4@MoS_2@DES-MIP$ , the thickness of the modified and imprinted layer is increased. Thus, the polymer formed by the polymerization reaction has been successfully grafted on the outer surface of the  $\text{Fe}_3\text{O}_4@MoS_2$ , which indicates that the magnetic surface molecularly imprinted polymer has been successfully prepared. In addition, the more cavities on the polymer particles can lead to the increase of the adsorption capacity and the mass transfer rate to release and recombine with the analyte.

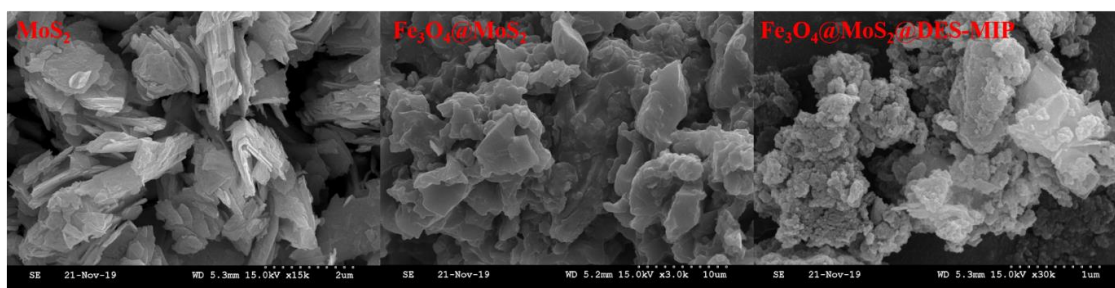


**Figure 2.** The FESEM images of the prepared  $\text{MoS}_2$ ,  $\text{Fe}_3\text{O}_4@MoS_2$ , and  $\text{Fe}_3\text{O}_4@MoS_2@DES-MIP$ .

## 2.2. Adsorption Capacity

### 2.2.1. Adsorption Isotherm

The static adsorption curves of  $\text{Fe}_3\text{O}_4@MoS_2@DES-MIP$  and non-imprinted polymer (NIP) at different temperatures (20, 30, and 40 °C) are shown in Figure 3. It can be seen from the figure that

its adsorption amount increases with increasing temperature. The reason for this may be that the MIP polymerizes at a higher temperature and has better adsorption capacity in a high temperature environment. Obviously, the equilibrium adsorption capacity of MIP is more than six times larger than that of NIP at the same temperature.

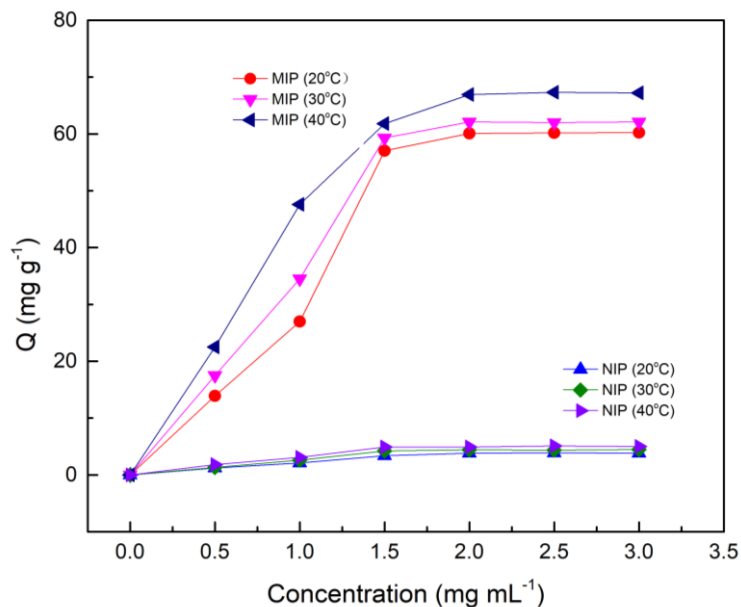


**Figure 3.** The static adsorption curves of  $\text{Fe}_3\text{O}_4@ \text{MoS}_2@ \text{DES-MIP}$  and  $\text{Fe}_3\text{O}_4@ \text{MoS}_2@ \text{DES-NIP}$ .

### 2.2.2. Adsorption Kinetics

The adsorption kinetic curve of MIP at 40 °C is shown in Figure 4. It can be observed that the adsorption capacity for EGCG by MIP is sharply increased before 30 min. However, it eventually tends to the equilibrium condition around 40 min, because the adsorption process needs to slowly enter the pores and combine with the recognition site. While there is no specific adsorption in the adsorption process of NIP, the adsorption amount is relatively small, and it had reached equilibrium in about 20 min.

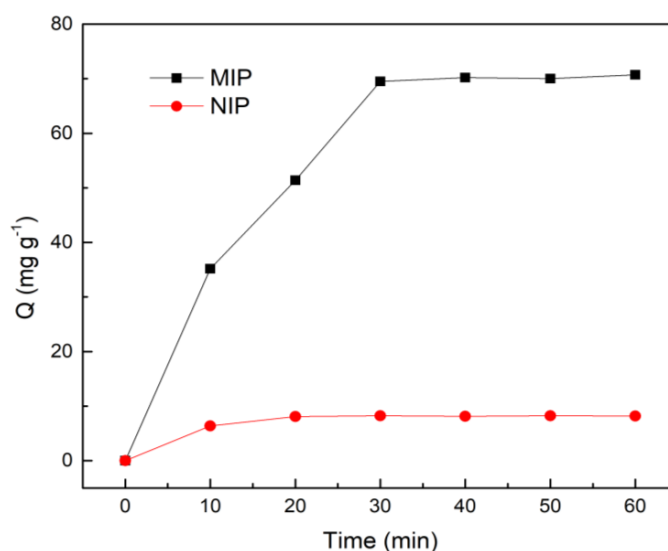


**Figure 4.** The adsorption kinetics curves of  $\text{Fe}_3\text{O}_4@ \text{MoS}_2@ \text{DES-MIP}$  and  $\text{Fe}_3\text{O}_4@ \text{MoS}_2@ \text{DES-NIP}$ .

### 2.2.3. Selective Adsorption Capacity

The selective adsorption capacity test of C, EC, EGC, ECG, and EGCG by MIP and NIP was prepared with EGCG as templates are shown in Figure 5. The result showed that when EGCG was applied as the template, the corresponding MIP exhibited excellent adsorption for its templated molecule of EGCG, with an adsorption capacity of  $70.5 \text{ mg} \times \text{g}^{-1}$ , while its adsorption capacities for C, EC, EGC, and ECG were greatly reduced, which are 25.5, 16.7, 16.9, and  $20.9 \text{ mg} \times \text{g}^{-1}$ ; the recoveries of those four analytes are 31.8%, 13.5%, 21.1%, and 26.2%, respectively. Similarly, MIP using EC as a template showed excellent selectivity for EC, and the adsorption of the other four analytes was very small. In addition, there was no significant difference in the adsorption amount of NIP to each substance, indicating that MIP has a higher selective adsorption capacity for a template molecule. The imprinting factor of the MIP with EGCG as a template was calculated to be 9.23 when the initial concentration of EGCG was  $2.00 \text{ mg} \times \text{mL}^{-1}$ . According to the comparison of the before and after of the MSPE process for the mixture of the five analytes, a significant decrease in the concentration of EGCG was found, while the concentrations of the other four substances remained almost unchanged. Therefore, the prepared  $\text{Fe}_3\text{O}_4@ \text{MoS}_2@ \text{DES-MIP}$  showed specific adsorption selectivity and EGCG can be identified well from structural analogs.

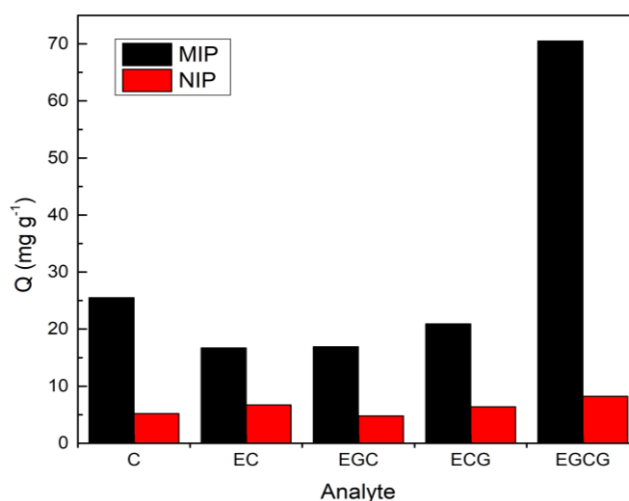


**Figure 5.** The selective adsorption capacity to the 5 catechins.  $\text{Fe}_3\text{O}_4@ \text{MoS}_2@ \text{DES-MIP}$  with EGCG template molecule and its corresponding NIP.

### 2.3. MIP Adsorption of EGCG in Green Tea

The chromatograms of the green tea extracts before and after  $\text{Fe}_3\text{O}_4@ \text{MoS}_2@ \text{DES-MIP}$  adsorption are shown in Figure 6. By comparing the chromatograms before and after adsorption, it was found that the peak area of EGCG changed obviously. It was calculated that about 97.9% of EGCG had been absorbed by MIP, while the concentration of other substances in green tea remained basically unchanged. Therefore, the MIP obtained in the experiment could selectively identify EGCG from green tea extractant and could be widely used in solid phase extraction of EGCG.

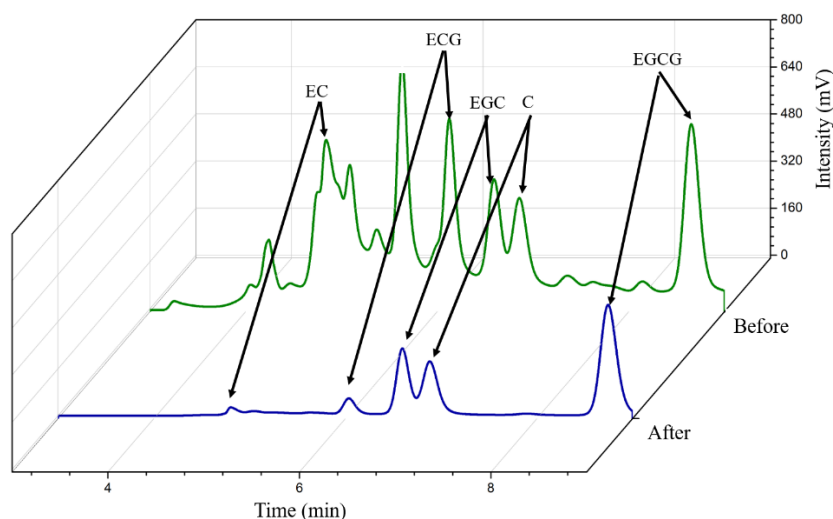


**Figure 6.** Chromatograms of green tea sample before and after MIP-SPE.

#### 2.4. Validation and Applications

The  $\text{Fe}_3\text{O}_4@\text{MoS}_2@\text{DES-MIP-MSPE-HPLC}$  method was evaluated, and the correlation coefficients ( $R^2$ ), limits of detection (LOD), and limits of quantification (LOQ) were obtained for the five catechins. Table 1 showed the calibration Curves, LOQs and LODs for the five analytes. Good linearities with  $R^2$  all above 0.990 were achieved, and the LODs from the five catechins were ranged from 0.36 to 1.20 mg/L. The accuracy and precision of the method were evaluated by performing three replicates of the fortified samples on the same and on different days, and the results are shown in Table 2. The relative standard deviations (RSD) for the intra-day and inter-day at the three levels of 10, 50, 100  $\mu\text{g} \times \text{mL}^{-1}$  were determined and all the RSD were less than 5.79%. The results showed that the reported method is reproducible and can be used for the analysis of the analytes in real samples. The repeatability of the prepared  $\text{Fe}_3\text{O}_4@\text{MoS}_2@\text{DES-MIP}$  was tested; the adsorbent after the extraction of the target molecule from green tea was collected by an extra magnet and applied to the extraction processes five times. The result showed that the target molecule could be extracted out again but the recoveries for the extracted amount were decreased from 98% to 55%.

**Table 1.** Calibration Curves ( $n = 5$ ), LODs, and LOQs for analytes.

Target	Equation	R2	LOQ (mg/L)	LOD (mg/L)
C	$Y = 128.85x - 64.5$	0.9992	0.60	0.20
EC	$Y = 103.71x - 19.48$	0.9991	1.20	0.40
EGC	$Y = 467.2x - 14.61$	0.9990	0.82	0.26
ECG	$Y = 207.36x - 25.26$	0.9990	0.36	0.10
EGCG	$Y = 197.96x - 33.25$	0.9994	0.50	0.15

**Table 2.** Magnetics solid-phase extraction method recoveries ( $n = 3$ ) and relative standard deviation values of analytes.

Analyte	Concentration ( $\mu\text{g/mL}$ )	Intra-Day		Inter-Day	
		Recovery (%)	RSD (%)	Recovery (%)	RSD (%)
C	10	88.1	2.01	82.4	3.62
	50	85.4	3.15	77.2	2.28
	100	84.8	4.4	75.9	4.4
EC	10	84.2	1.91	78.4	2.96
	50	82.4	2.54	76.8	3.25
	100	80.7	5.79	74.7	4.01
EGC	10	84	2.09	76.2	2.85
	50	80.3	2.84	74.9	4.32
	100	79.5	4.22	73.3	5.48
ECG	10	84	2.09	76.2	2.85
	50	80.3	2.84	74.9	4.32
	100	79.5	4.22	73.3	5.48
EGCG	10	98.6	2.09	92.1	2.85
	50	95.7	2.84	88.9	4.32
	100	90.4	2.01	85.3	3.62

### 3. Materials and Methods

#### 3.1. Reagents and Materials

Vinyl pyrrolidone (VP), iron (III) chloride hexahydrate ( $\text{FeCl}_3 \cdot 6\text{H}_2\text{O}$ ), sodium acetate, malonic acid (MA), and molybdenum disulfide ( $\text{MoS}_2$ ) were purchased from Sigma Chemical Co. (St. Louis, MO, USA). Acetic acid and ethylene glycol were procured from Duskan Pure Chemical (Kyungki-do, Korea). Methanol and ethanol were acquired from Fisher Scientific (Seoul, Korea). Ammonium persulfate (APS), 3-methacryloxypropyltrimethoxysilane (MPS), Ethylene glycol dimethacrylate (EGDMA), and 2-methylpropionitrile (AIBN) were purchased from Daejung Chemicals & Metals (Gyeonggido, Korea). The standard chemicals of (+)-catechin (C,  $\geq 98\%$ ), (–)-epicatechin (EC,  $\geq 90\%$ ), (–)-epigallocatechin (EGC,  $\geq 95\%$ ), (–)-epicatechin gallate (ECG,  $\geq 95\%$ ), and (–)-epigallocatechin gallate (EGCG,  $\geq 98\%$ ) were supplied by Tokyo Chemical Industry (Tokyo, Japan). All other solvents used in the experiment were either of HPLC or analytical grade.

#### 3.2. Instrumentation and Conditions

The chromatographic analysis was carried on a YL9100 HPLC System (Incheon, Korea) that consisted of three parts: a YL9110 quaternary pump, an injector with a 20 mL sample loop, and a UV-visible dual channel detector. The data acquisition system was effectuated with the Autochro-2000 software (Younglin, Korea). HPLC separation was carried out with the mobile phase of water/methanol/acetic acid (70:30:0.01,  $v/v/v$ ) with a flow rate of 0.8 mL/min, and an OptimaPak C18 column (5  $\mu\text{m}$ ,  $250 \times 4.6$  mm, id, RS tech Corporation, Daejeon, Korea) was applied to the stationary phase. The injection volume was 10  $\mu\text{L}$ , the column temperature was kept at 30  $^\circ\text{C}$ , and UV-vis detector was set at a wavelength of 278 nm.

The characterizations of the systemized materials were performed with a field emission scanning electron microscopy (FE-SEM S-4200, Hitachi, Ontario, Canada) and Fourier transform infrared spectra (FTIR, Vertex 80 V Bruker, Billerica, MA, USA). The morphology evaluation was examined by FE-SEM S-4200 with an acceleration voltage of 15 kV (pixel size: 0.5 nm) to observe the structure and size changes of the MIP. FTIR was performed over the range of 4000–400  $\text{cm}^{-1}$ , at a scan rate of 20 scans/min using a KBr pellet to analyze the graft bonding of the polymer surface at each stage of the experiment.



### 3.3. Preparation of DESs

The VP-based DESs were synthesized by the heating method according to Fu's work [22]. Briefly, 0.1 mol VP and 0.1 mol MA were placed in a 100-mL round-bottom flask, the mixture was constantly stirred and kept in a water bath with the temperature set at 80 °C. The DES could be obtained until the mixture becomes evenly and clear.

### 3.4. Preparation of $Fe_3O_4@MoS_2$ -MPS Nanoparticles

$Fe_3O_4@MoS_2$  core-shell composites were prepared according to Chen's method [21], but there was a slight modification. 12.9 g  $FeCl_3 \cdot 6H_2O$  and 2.94 g sodium acetate were added into a beaker with 100 mL ethylene glycol, then 3.137 g  $MoS_2$  nanoparticles were dispersed in the mixture homogeneously with the help of ultrasound sonication for 2 h with a 20 min intermittent time interval. Following, the mixture was transferred to a 200-mL Teflon-lined stainless-steel autoclave and sealed to heat at 150 °C for 10 hours. After the mixture was cooled down to room temperature, the obtained black product was rinsed with distilled water several times with a centrifuge and the synthesized  $Fe_3O_4@MoS_2$  nanoparticles were collected by an extra magnet.

To prepare the  $Fe_3O_4@MoS_2$  nanoparticles modified with MPS, the obtained  $Fe_3O_4@MoS_2$  nanoparticles were dispersed in 50 mL of anhydrous toluene containing 5 mL of MPS, and the mixture was stirred for 8 h at 60 °C. The  $Fe_3O_4@MoS_2$  microspheres modified by MPS ( $Fe_3O_4@MoS_2$ -MPS) were washed respectively with DMSO and ethanol several times, then collected by an extra magnet.

### 3.5. Preparation of $Fe_3O_4@MoS_2$ @DES-MIP

The DES-MIPs were prepared via the surface imprinted polymerization method as follows: A 1 mg template of EGCG and 1 mmol of functional monomer of DES were added to the via and then they were dispersed in toluene (15 ml) by sonication, then the mixture stood at room temperature for 6 hours before use. Thirty milligrams of the prepared  $Fe_3O_4@MoS_2$ -MPS, 2 mmol cross-linker of EGDMA, 10 mg initiator of AIBN, and 1 mL porogen of ethanol–water mixture with the volume ratio of 9:1 (*v/v*) were all placed together in a mixture and dissolved under ultrasonic agitation for 5 min. Next, the pre-assembly solution was dropped into the above solution under a  $N_2$  gas sweep, and then mechanically stirred at 60 °C overnight. After the polymerization was completed, the products were repeatedly washed with acetonitrile and deionized water until the supernatant was transparent, then methanol-acetic acid (volume ratio 9:1) was used to finally remove the template molecules. Finally, it was washed with methanol to neutrality and dried under vacuum at 50 °C to obtain the  $Fe_3O_4@MoS_2@DES$ -MIP; the schematic illustration of the preparation of  $Fe_3O_4@MoS_2@DES$ -MIP is shown in Figure 7.

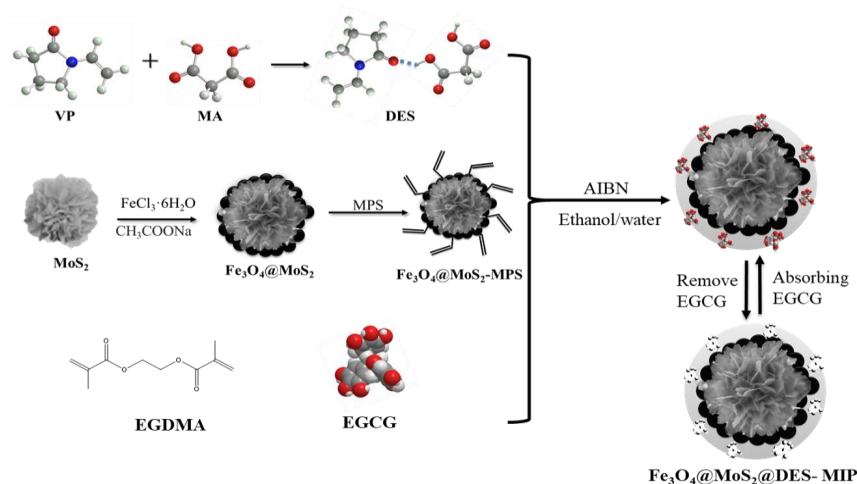


**Figure 7.** Schematic of the preparation of DES and  $Fe_3O_4@MoS_2@DES$ -MIP.



The same method was applied to the preparation of DES-based magnetic non-imprinted polymers ( $\text{Fe}_3\text{O}_4@ \text{MoS}_2@ \text{DES-NIP}$ ) and magnetic imprinted polymers ( $\text{Fe}_3\text{O}_4@ \text{MoS}_2\text{-MIP}$ ) without adding the template of EGCG and DES, respectively.

### 3.6. Sample Pretreatment

The standard products of the five kind of catechins were accurately weighed and the standard stock solutions of them were prepared with deionized water. The standard stock solution was diluted with deionized water to obtain standard solutions of 1, 5, 10, 50, 100, and 200  $\mu\text{g} \times \text{mL}^{-1}$ , respectively, then the standard curve of them was obtained with the help of HPLC.

After drying the Green tea in an oven (50 °C) and grinding it to a powder, 1 g powder of the green tea sample was weighed and soaked in 90 °C distilled water for 20 mins. After centrifugal separation, the suspension was then filtered to obtain the extraction samples; finally, the sample solution was filtered through a 0.45  $\mu\text{L}$  nylon membrane before being applied further.

### 3.7. Absorption Capacity Test of $\text{Fe}_3\text{O}_4@ \text{MoS}_2@ \text{DES-MIP}$

#### 3.7.1. Adsorption Thermodynamic Experiment

A series of EGCG aqueous solutions (0.5, 1.0, 1.5, 2.0, 2.5, and 3.0  $\text{mg} \times \text{mL}^{-1}$ ) were prepared, and 15 mg of MIP or NIP was added to the EGCG solution of 3.00 mL. They were then shaken at a constant temperature for 120 min at different temperatures (20, 30 and 40 °C). After fully adsorbed, the adsorbed solution was separated magnetically, and its peak area was determined by HPLC with the help of EGCG standard curve. The EGCG concentration in the solution after adsorption was measured three times in parallel and then determined. The adsorption amount of EGCG was calculated by the Formula (1).

$$Q = \frac{(C_0 - C_v) * V}{m} \quad (1)$$

In the formula,  $Q$  ( $\text{mg} \times \text{g}^{-1}$ ) is the adsorption amount of the target substance by the polymer,  $C_0$  ( $\text{mg} \times \text{mL}^{-1}$ ) and  $C_v$  ( $\text{mg} \times \text{mL}^{-1}$ ) are the initial concentrations of the target substance and the concentration of the standard solution after shaking for 120 min,  $V$  (mL) is the Volume of the added standard solution, and  $m$  (g) is the mass of the adsorbent of  $\text{Fe}_3\text{O}_4@ \text{MoS}_2@ \text{DES-MIP}$ .

#### 3.7.2. Adsorption Kinetics Experiment

One-hundred milligrams of  $\text{Fe}_3\text{O}_4@ \text{MoS}_2@ \text{DES-MIP}$  was added into 10 mL of EGCG solution with the concentration of 2.0  $\text{mg mL}^{-1}$  with consistent shaking at 40 °C, and then the samples were separated and collected at different times. The contraction in the solution after adsorption was determined by HPLC. The adsorption amount of EGCG was calculated by Formula (1).

#### 3.7.3. Selection Adsorption Experiments

Fifteen milligrams of MIPs were added to 3.0 mL of C, EC, EGC, ECG, and EGCG solutions (all at the concentration of 2.0  $\text{mg mL}^{-1}$ ) while constantly shaking at 30 °C for 120 min, respectively. After it was fully adsorbed, the supernatants were separated from the polymer by an external magnet and then discarded. The equilibrium adsorption capacity of  $\text{Fe}_3\text{O}_4@ \text{MoS}_2@ \text{DES-MIP}$  for the five substances was calculated and measured in parallel three times. Repeat the above steps to determine the adsorption capacity of these five substances with the imprinted polymer using EC as a template. The equilibrium adsorption capacity is calculated by Formula (1); the recognition specificity of the MIP is evaluated using the imprinting factor ( $\alpha$ ); and the value of  $\alpha$  is calculated by Formula (2)

$$\alpha = \frac{Q_{MIP}}{Q_{NIP}} \times 100\% \quad (2)$$

In the formula,  $Q_{MIP}$  and  $Q_{NIP}$  are the adsorption amounts (mg/g) of GA to imprinted and non-imprinted polymers, respectively.

In addition, 3.0 mL of a mixed standard solution of C, EC, EGC, ECG, and EGCG (all with a concentration of  $2.0 \text{ mg} \times \text{mL}^{-1}$ ) was shaken with the addition of 15 mg of MIP at  $30^\circ\text{C}$  for 120 min, and then analyzed by HPLC. The concentration of each component in the solution before and after adsorption was evaluated to evaluate the difference in the selective adsorption abilities of MIP to these five structural analogs.

#### 4. Conclusions

The magnetic surface molecularly imprinted polymer of  $\text{Fe}_3\text{O}_4@MoS_2@DES\text{-MIP}$  was successfully synthesized with EGCG as a template,  $\text{Fe}_3\text{O}_4@MoS_2$  as a base, and a new type of DES as a functional monomer, and it was applied in the MSPE-HPLC method for the selective recognition and separation of five kind of catechins (C, EC, EGC, ECG, and EGCG) in green tea. The results show that the adsorption capacity of MIP was about six times higher than that of NIP. The saturated adsorption capacity of EGCG was significantly higher than that of the other four catechins, which indicates that MIP has a specific selective recognition of EGCG. It was found that MIP could adsorb more than 98% of EGCG in green tea extractant and could be applied in the MSPE process. The application of  $MoS_2$  combined with  $Fe_3O_4$  and the application of green solvent of DES instead of the traditional functional monomer may provide further exploration in the preparation of MIP.

**Author Contributions:** Conceptualization, W.M. and K.H.R.; methodology, W.M. and K.H.R.; software, W.M. and K.H.R.; validation, W.M. and K.H.R.; formal analysis, W.M. and K.H.R.; investigation, W.M. and K.H.R.; resources, W.M. and K.H.R.; data curation, W.M. and K.H.R.; writing—original draft preparation, W.M. and K.H.R.; writing—review and editing, W.M. and K.H.R.; visualization, W.M. and K.H.R.; supervision, K.H.R.; project administration, K.H.R.; funding acquisition, K.H.R. All authors have read and agreed to the published version of the manuscript.

**Funding:** This research was funded by the National Research Foundation of Korea (NRF) grant funded by the Korea government (MSIT), grant number No.NRF-2019R1A2C1010032.

**Acknowledgments:** All this work was supported by the National Research Foundation of Korea (NRF) grant funded by the Korea government (MSIT) (No.NRF-2019R1A2C1010032).

**Conflicts of Interest:** The authors declare no conflict of interest.

#### References

1. Suzuki, T.; Pervin, M.; Goto, S.; Isemura, M.; Nakamura, Y. Beneficial effects of tea and the green tea catechin epigallocatechin-3-gallate on obesity. *Molecules* **2016**, *21*, 1305. [[CrossRef](#)] [[PubMed](#)]
2. Selvi, I.K.; Nagarajan, S. Separation of catechins from green tea (*Camellia sinensis* L.) by microwave assisted acetylation, evaluation of antioxidant potential of individual components and spectroscopic analysis. *LWT* **2018**, *91*, 391–397. [[CrossRef](#)]
3. Fujioka, K.; Iwamoto, T.; Shima, H.; Tomaru, K.; Saito, H.; Ohtsuka, M.; Yoshidome, A.; Kawamura, Y.; Manome, Y. The powdering process with a set of ceramic mills for green tea promoted catechin extraction and the ROS inhibition effect. *Molecules* **2016**, *21*, 474. [[CrossRef](#)]
4. Mawson, D.H.; Jeffrey, K.L.; Teale, P.; Grace, P.B. Development and validation of a high-throughput assay for the quantification of multiple green tea-derived catechins in human plasma. *Biomed. Chromatogr.* **2018**, *32*, e4319. [[CrossRef](#)] [[PubMed](#)]
5. Tang, W.; Row, K.H. Evaluation of  $CO_2$ -induced azole-based switchable ionic liquid with hydrophobic/hydrophilic reversible transition as single solvent system for coupling lipid extraction and separation from wet microalgae. *Bioresour. Technol.* **2020**, *296*, 122309. [[CrossRef](#)] [[PubMed](#)]
6. Wang, K.; Chen, Q.; Lin, Y.; Yu, S.; Lin, H.; Huang, J.; Liu, Z. Separation of catechins and O-methylated (–)-epigallocatechin gallate using polyamide thin-layer chromatography. *J. Chromatogr. B* **2016**, *1017*, 221–225. [[CrossRef](#)]

7. Ma, W.; Dai, Y.; Row, K.H. Molecular imprinted polymers based on magnetic chitosan with different deep eutectic solvent monomers for the selective separation of catechins in black tea. *Electrophoresis* **2018**, *39*, 2039–2046. [[CrossRef](#)]
8. Šilarová, P.; Česlová, L.; Meloun, M. Fast gradient HPLC/MS separation of phenolics in green tea to monitor their degradation. *Food Chem.* **2017**, *237*, 471–480. [[CrossRef](#)]
9. Sökmen, M.; Demir, E.; Alomar, S.Y. Optimization of sequential supercritical fluid extraction (SFE) of caffeine and catechins from green tea. *J. Supercrit. Fluid.* **2018**, *133*, 171–176. [[CrossRef](#)]
10. Fiori, J.; Pasquini, B.; Caprini, C.; Orlandini, S.; Furlanetto, S.; Gotti, R. Chiral analysis of theanine and catechin in characterization of green tea by cyclodextrin-modified micellar electrokinetic chromatography and high performance liquid chromatography. *J. Chromatogr. A* **2018**, *1562*, 115–122. [[CrossRef](#)]
11. Criscenti, G.; De Maria, C.; Longoni, A.; Van Blitterswijk, C.A.; Fernandes, H.A.; Vozzi, G.; Moroni, L. Soft-molecular imprinted electrospun scaffolds to mimic specific biological tissues. *Biofabrication* **2018**, *10*, 045005. [[CrossRef](#)] [[PubMed](#)]
12. Vozzi, G.; Morelli, I.; Vozzi, F.; Andreoni, C.; Salsedo, E.; Morachioli, A.; Giusti, P.; Ciardelli, G. SOFT-MI: A novel microfabrication technique integrating soft-lithography and molecular imprinting for tissue engineering applications. *Biotechnol. Bioeng.* **2010**, *106*, 804–817. [[CrossRef](#)] [[PubMed](#)]
13. Jia, M.; Zhang, Z.; Li, J.; Ma, X.; Chen, L.; Yang, X. Molecular imprinting technology for microorganism analysis. *TrAC-Trend. Anal. Chem.* **2018**, *106*, 190–201. [[CrossRef](#)]
14. Ma, W.; An, Y.; Row, K.H. Preparation and evaluation of a green solvent-based molecularly imprinted monolithic column for the recognition of proteins by high-performance liquid chromatography. *Analyst* **2019**, *144*, 6327–6333. [[CrossRef](#)] [[PubMed](#)]
15. Wackerlig, J.; Lieberzeit, P.A. Molecularly imprinted polymer nanoparticles in chemical sensing—Synthesis, characterisation and application. *Sensor. Actuat. B-Chem.* **2015**, *207*, 144–157. [[CrossRef](#)]
16. Rechichi, A.; Cristallini, C.; Vitale, U.; Ciardelli, G.; Barbani, N.; Vozzi, G.; Giusti, P. New biomedical devices with selective peptide recognition properties. Part 1: Characterization and cytotoxicity of molecularly imprinted polymers. *J. Cell. Mol. Med.* **2007**, *11*, 1367–1376. [[CrossRef](#)]
17. BelBruno, J.J. Molecularly imprinted polymers. *Chem. Rev.* **2018**, *119*, 94–119. [[CrossRef](#)]
18. Wang, H.; Liu, Y.; Yao, S.; Zhu, P. Selective recognition of dicyandiamide in bovine milk by mesoporous silica SBA-15 supported dicyandiamide imprinted polymer based on surface molecularly imprinting technique. *Food Chem.* **2018**, *240*, 1262–1267. [[CrossRef](#)]
19. Fu, N.; Li, L.; Liu, K.; Kim, C.K.; Li, J.; Zhu, T.; Li, J.; Tang, B. A choline chloride-acrylic acid deep eutectic solvent polymer based on Fe<sub>3</sub>O<sub>4</sub> particles and MoS<sub>2</sub> sheets (poly (ChCl-AA DES)@Fe<sub>3</sub>O<sub>4</sub>@MoS<sub>2</sub>) with specific recognition and good antibacterial properties for β-lactoglobulin in milk. *Talanta* **2019**, *197*, 567–577. [[CrossRef](#)]
20. Xiao, R.; Wang, S.; Ibrahim, M.H.; Abdu, H.I.; Shan, D.; Chen, J.; Lu, X. Three-dimensional hierarchical frameworks based on molybdenum disulfide-graphene oxide-supported magnetic nanoparticles for enrichment fluoroquinolone antibiotics in water. *J. Chromatogr. A* **2019**, *1593*, 1–8. [[CrossRef](#)]
21. Chen, Y.; Song, B.; Tang, X.; Lu, L.; Xue, J. Ultrasmall Fe<sub>3</sub>O<sub>4</sub> nanoparticle/MoS<sub>2</sub> nanosheet composites with superior performances for lithium ion batteries. *Small* **2014**, *10*, 1536–1543. [[CrossRef](#)] [[PubMed](#)]
22. Fu, N.; Li, L.; Liu, X.; Fu, N.; Zhang, C.; Hu, L.; Li, D.; Zhu, T. Specific recognition of polyphenols by molecularly imprinted polymers based on a ternary deep eutectic solvent. *J. Chromatogr. A* **2017**, *1530*, 23–34. [[CrossRef](#)] [[PubMed](#)]
23. Li, X.; Dai, Y.; Row, K.H. Preparation of two-dimensional magnetic molecularly imprinted polymers based on boron nitride and a deep eutectic solvent for the selective recognition of flavonoids. *Analyst* **2019**, *144*, 1777–1788. [[CrossRef](#)] [[PubMed](#)]
24. Chen, J.; Liu, M.; Wang, Q.; Du, H.; Zhang, L. Deep eutectic solvent-based microwave-assisted method for extraction of hydrophilic and hydrophobic components from radix salviae miltiorrhizae. *Molecules* **2016**, *21*, 1383. [[CrossRef](#)] [[PubMed](#)]
25. Liu, H.; Jiang, L.; Lu, M.; Liu, G.; Li, T.; Xu, X.; Li, L.; Lin, H.; Lv, J.; Huang, X.; et al. Magnetic Solid-Phase Extraction of Pyrethroid Pesticides from Environmental Water Samples Using Deep Eutectic Solvent-type Surfactant Modified Magnetic Zeolitic Imidazolate Framework-8. *Molecules* **2019**, *24*, 4038. [[CrossRef](#)]
26. Zhang, Y.; Cao, H.; Huang, Q.; Liu, X.; Zhang, H. Isolation of transferrin by imprinted nanoparticles with magnetic deep eutectic solvents as monomer. *Anal. Bioanal. Chem.* **2018**, *410*, 6237–6245. [[CrossRef](#)]

27. Xu, K.; Wang, Y.; Wei, X.; Chen, J.; Xu, P.; Zhou, Y. Preparation of magnetic molecularly imprinted polymers based on a deep eutectic solvent as the functional monomer for specific recognition of lysozyme. *Microchim. Acta.* **2018**, *185*, 146. [[CrossRef](#)]
28. Li, X.; Row, K.H. Preparation of deep eutectic solvent-based hexagonal boron nitride-molecularly imprinted polymer nanoparticles for solid phase extraction of flavonoids. *Microchim. Acta.* **2019**, *186*, 753. [[CrossRef](#)]
29. Li, L.; Liu, K.; Xing, H.; Li, X.; Zhang, Q.; Han, D.; He, H.; Yan, H.; Tang, B. Deep eutectic solvents functionalized polymers for easily and efficiently promoting biocatalysis. *J. Catal.* **2019**, *374*, 306–319. [[CrossRef](#)]

**Sample Availability:** Not available.



© 2020 by the authors. Licensee MDPI, Basel, Switzerland. This article is an open access article distributed under the terms and conditions of the Creative Commons Attribution (CC BY) license (<http://creativecommons.org/licenses/by/4.0/>).